Defence Science Journal, Vol. 70, No. 4, July 2020, pp. 374-382, DOI : 10.14429/dsj.70.15040

A Case-based Online Trajectory Planning Method of Autonomous Unmanned Combat Aerial Vehicles with Weapon Release Constraints

Jiayu Tang*, Xiangmin Li, Jinjin Dai, and Ning Bo

Naval Aviation University, China
**E-mail: 342118507@qq.com*

ABSTRACT

As a challenging and highly complex problem, the trajectory planning for unmanned combat aerial vehicle (UCAV) focuses on optimising flight trajectory under such constraints as kinematics and complicated battlefield environment. An online case-based trajectory planning strategy is proposed in this study to achieve rapid control variables solution of UCAV flight trajectory for the of delivery airborne guided bombs. Firstly, with an analysis of the ballistic model of airborne guided bombs, the trajectory planning model of UCAVs is established with launch acceptable region (LAR) as a terminal constraint. Secondly, a case-based planning strategy is presented, which involves four cases depending on the situation of UCAVs at the current moment. Finally, the feasibility and efficiency of the proposed planning strategy is validated by numerical simulations, and the results show that the presented strategy is suitable for UCAV performing airborne guided delivery missions in dynamic environments.

Keywords: Unmanned combat air vehicle; UCAV; Trajectory planning; Receding horizon control; Threat environment

1. INTRODUCTION

In respect of military mission planning of unmanned aerial vehicles (UAVs), a critical problem is to obtain a path that allows UAVs to arrive at a pre-assigned target point considering the dynamics of vehicles with obstacles, collisions and threats avoidance[1]. Under this circumstance, online real-time trajectory planning of unmanned combat aerial vehicle (UCAVs) has become a hotspot.

At present, there have been many trajectory planning methods proposed for UAVs with the improvement of airborne computational capabilities[2]. The specific algorithms include cuckoo search[3], moth search algorithm[4], chaotic artificial bee colony[5], biogeography-based optimisation (BBO)[6], intelligent water drops optimisation[7] and other optimal control methods. In recent years, the focus of more and more studies has shifted to applying optimal control methods to solve trajectory planning problems. Nevertheless, it is virtually difficult to obtain a rapid solution of optimisation methods due to the unrealistic prospect of working out analytical solutions. Therefore, numerical techniques have been applied to address the trajectory planning problems[8]. Numerical methods can be classed into two types, direct methods and indirect methods[9].

Zhang[10], *et al*. proposed a real-time trajectory planning framework using inverse dynamics optimisation method in combination with receding horizon control. Zhu[11], *et al.* suggested a Chaotic Predator-Prey Biogeography-based Optimisation (CPPBBO) approach to generate optimal or quasi-optimal flight path. Duan[12], *et al*. put forward an artificial neural network (ANN) in combination with imperialist competitive algorithm (ICA) for globally optimal trajectories. Curiac[13], *et al.* adopted the 3D Arnold's cat map to surveil the adversarial situation for path planning. Wang[8], *et al.* proposed an improved version of bat algorithm (BA) for UCAV optimal trajectories.

The relevant studies have been conducted to solve the problem with UCAV trajectory planning under desirable scenarios where only static threats are taken into account. However, the battlefield is highly complex and dynamic, which makes it necessary to develop an online trajectory planning algorithm for coping with pop-up mobile threats and targets. Besides, to ensure that the air-to-ground attack mission can be performed with success, UCAVs are supposed to arrive at the launch acceptable area of airborne guided bombs.

In this paper, we discuss the problem of quickly finding a feasible flight path for UCAV from a predetermined starting point to the LAR and releasing airborne guided bombs to complete ground attacking. The flight path is required to be sufficiently smooth to satisfy the kinematic constraints of UCAVs while avoiding certain no-fly zones and highly-risky regions.

2. TRAJECTORY PLANNING MODEL OF UCAV WITH WEAPON RELEASE CONSTRAINTS

To address the issues of path planning for UCAVs with weapon delivery demands, a mathematical trajectory planning model with weapon release constraints is proposed in this

Received : 02 September 2019, Revised : 20 April 2020
Accepted : 21 May 2020, Online published : 13 July 2020

section. Firstly, the kinematic model of UCAV is introduced. Secondly, based on an analysis of the ballistic model of guided bombs equipped in UCAVs, LAR is obtained to serve as a terminal constraint for trajectory planning.

2.1 Kinematic Model of UCAV

Compared with tiltrotors, fixed-wing UCAVs demonstrate various advantages. Firstly, they can fly longer missions with a significantly higher velocity. Secondly, they are more reliable and suitable for highly complicated and dynamic missions, such as the suppression of enemy air defences and ground attack. It is assumed that each UCAV is equipped with a high-performance low-level flight control system that ensures the stability of roll, pitch and yaw maneuvers with altitude holding ability. Explicit flight speed, turn rate and climb rate are treated as the control inputs[14].

Eqn. (1) represents the kinematic features of UCAV as a mass point.

$$\begin{cases} \dot{x} = u_1 \cos\psi \\ \dot{y} = u_1 \sin\psi \\ \dot{\psi} = u_2 \\ \dot{h} = u_3 \end{cases}, \tag{1}$$

where $p = (x, y, h)$ represents the three-dimensional inertial coordinate of UCAV, ψ indicates the heading angle, $u = [u_1, u_2, u_3]^T$ denotes the control variable of the trajectory, the components of which are the control variables of airspeed, turning rate and climb rate, i.e. $u_1 = V$, $u_2 = \omega$, and $u_3 = \ell$.

2.2 Solution of LAR of Airborne Guided Bombs

For the sake of attack accuracy and enhance striking performance, it is necessary for guided bombs to be released in a specified and limited area, which is referred to as the release area[8]. Within this area, when UCAV releases guided bombs with satisfied constraints, the bombs can hit targets to the predefined precision, otherwise they are highly likely to miss the targets with a great possibility. Therefore, the LAR of airborne weapons needs to be identified before trajectory planning, and it is supposed to be taken as a terminal constraint for the occupation of the UCAV before attacking.

2.2.1 Motion Model of Airborne Guided Bombs

2.2.1.1 Ballistic Model of Guided Bombs

The aim of obtaining the LAR is to identify the ballistic trajectory. It is worth noting that guided bombs glide without stimulus during the flight. For the convenience of modelling, three assumptions are made as follows.

(i) Bombs glide under a standard atmospheric condition with no external interference factors.
(ii) Rotatory inertia of bombs is ignored, which means that the rotations around the particle are excluded from study here.
(iii) The measurement and control systems of bombs operate accurately without any delay.

The kinematic equations of guided bombs are identical to Eqn. (1), and the dynamic model is

$$\begin{cases} \dot{V}_B = -D/m_B - g\sin\gamma_B \\ \dot{\theta}_B = g(n_d - \cos\gamma_B)/V_B \\ \dot{\xi}_B = -gn_t/(V_B\cos\gamma_B) \end{cases} \tag{2}$$

where V_B denotes the speed of the guided bomb; m_B indicates its mass; g stands for the gravity acceleration; ξ_B and γ_B refer to the deflection angle and flight path angle of the bomb respectively; n_d and n_t represent the tangential and normal component of the load factor; D denotes the relative distance, i.e.

$$D = \sqrt{(s_m - s_T)^2 + (l_m - l_T)^2 + (p_m - p_T)^2} \tag{3}$$

and (l_m, p_m, s_m) represents the bomb position after release, and (l_T, p_T, s_T) refers to the target position.

2.2.1.2 Guidance Law Model

UCAVs are equipped with laser guided bombs which are technically mature and lightweight. Without roll angle and its velocity, the three-dimensional motion of guided bombs is decoupled into motions in the diving and turning planes.

The velocity of the line-of-sight angle is

$$\begin{cases} q_d = \arctan\left((s_m - s_T)/(l_m - l_T)\right) \\ q_r = \arctan\left(-(p_m - p_T)/D\right) \end{cases}, \tag{4}$$

q_d and q_r denote the elevation angle in the diving plane and the azimuth angle in the turning plane.

Airborne bombs are guided by the traditional proportional guidance law, i.e.

$$\begin{cases} n_d = K_d V_B \dot{q}_d / g + \cos\gamma_B \\ n_t = -K_t (V_B \dot{q}_t \cos\gamma_B)/g \end{cases} \tag{5}$$

where K_d and K_t refer to proportional gains.

2.2.2 Launch Acceptable Region

In order to identify the acceptable release area, it is necessary to first calculate the edges of landing footprint of airborne guided bombs, which consists of the impact points of limiting range (optimal range). Then, the landing footprint area is transformed into LAR in line with the transformation process[15].

The detailed algorithm[11] to acquire the LAR is presented in Fig. 1.

In Fig. 1, the range of off-axis bearing angles is limited to between $-\theta_{max}$ and θ_{max}, and

$$\Delta\theta = 2\theta_{max}/N_\theta \tag{6}$$

represents the average interval length per step.

2.3 Trajectory Planning Constraints

The constraints of trajectory planning include boundary constraints and process constraints.

2.3.1 Boundary Constraints

Boundary constraints involve initial constraints and terminal constraints.

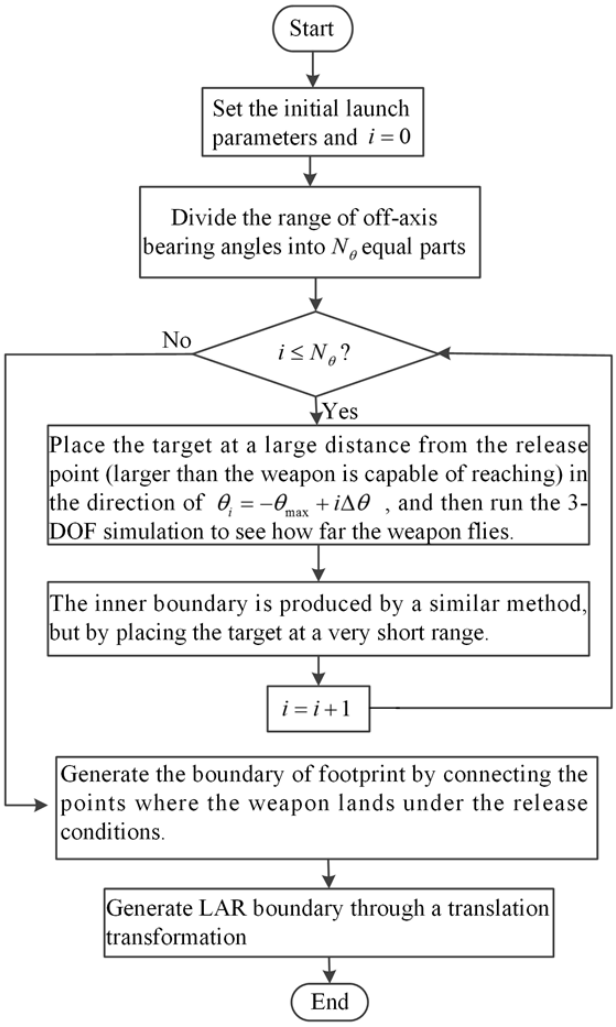

Figure 1. Flow chart of acquiring LAR.

2.3.1.1 Initial Constraints

Initial constraints are

$$\begin{cases} x(t_s)=x_s, y(t_s)=y_s, \\ h(t_s)=h_s, \psi(t_s)=\psi_s, \\ u_1(t_s)=V_s, u_2(t_s)=\omega_s, u_3(t_s)=\ell_s. \end{cases} \tag{7}$$

2.3.1.2 Terminal Constraints

To improve the precision of attack, the LAR of airborne guided bombs is treated as the main terminal constraint. Once it enters the LAR, the UCAV starts self-adjustment to meet the release conditions[10].

The position of the center of LAR is $(\overline{x}, \overline{y})$, i.e.

$$\begin{cases} \overline{x} = \left(\sum_{i=1}^{N_p} x_i\right) \Big/ N_p \\ \overline{y} = \left(\sum_{i=1}^{N_p} y_i\right) \Big/ N_p \end{cases}, \tag{8}$$

where (x_i, y_i) indicates the i -th vertex of LAR envelope, and N_p denotes the number of vertices. Therefore, the terminal constraint is transformed into

$$\begin{cases} |x_f - \overline{x}| \le \varepsilon_x \\ |y_f - \overline{y}| \le \varepsilon_y, \\ |h_f - \overline{h}| \le \varepsilon_h \end{cases} \tag{9}$$

where ε_x , ε_y and ε_h denote the permitted distance errors along the axis as determined by the range of the LAR, while (x_f, y_f, h_f) represents the terminal point.

Moreover, the state constraints of the UCAV to launch airborne bombs are

$$\begin{cases} V(t_f)=V_f \\ \psi(t_f)=\xi_f \end{cases}, \tag{10}$$

where t_f refers to the terminal time.

2.3.2 Process Constraints

During the flight, the process constraints that need to be satisfied include maneuverability and battlefield constraints.

2.3.2.1 Maneuverability Constraints

Maneuverability constraints involve the restrictions imposed on velocity, acceleration, heading angles and the minimum turning radius, as shown below.

$$\begin{cases} V_{\min} \le u_1 \le V_{\max}, \\ a_{\min} \le a \le a_{\max}, \\ \omega_{\min} \le u_2 \le \omega_{\max}, \\ \gamma_{\min} \le u_3 \le \gamma_{\max}, \\ r \ge r_{\min} = \dfrac{V}{\omega_{\max}}, \end{cases} \tag{11}$$

where a indicates the acceleration of the UCAV.

2.3.2.2 Battlefield constraints

Coordinated ground attack missions are known for complex battlefield with both topographic obstacles and such violent threats as integrated air defenses systems (IADS). The threats are categorised into hard and soft threats[14].

(a) Hard Threats : It include topographic obstacles (such as hills and buildings) and other no-fly zones.

Elliptical cylinders work as a basic shape of hard threats. There are M_1 hard threats $H_m = \langle A_m, P_m \rangle, m = 1, \cdots, M_1$, where A_m represents the center coordinate of the ellipsoid and P_m indicates the shape matrix. Therefore, the collision function of UCAV is

$$F_m(p(h)) = 1 - (p(h) - A_m(h))^T P_m^{-1}(h)(p(h) - A_m(h)), \tag{12}$$

where $p(h) = (x, y)$ refers to the 2D position of the UAV with its flight height h . $F_m(p(h)) < 0$ indicates that the UCAV is capable to keep flying without considering the hard threat H_m.

(b) Soft Threats : It refer to the safety threats related to air defense weapons, such as IADS and air defense artillery.

Different from the complete avoidance of hard threats, UCAV ought to maintain a safe distance from soft threats. There are M_2 soft threats, and the threat function of the j-th $(j=1,\cdots,M_2)$ soft threat is

$$Th_j\left(p(h)\right)=\lambda(h)\exp\left[-\frac{1}{2}\left(p(h)-B_j(h)\right)^T Q_j^{-1}(h)\left(p(h)-B_j(h)\right)\right], \quad (13)$$

where $\lambda(h)$ indicates the threat intensity related to the flight height h, while $B_j(h)$ and $Q_j(h)\geq 0$ denote the position and threat range respectively. When the UCAV flies at a constant altitude, or the threat intensity varies little as the flight height changes, $\lambda(h)=1$.

$Th_j\left(p(h)\right)$ indicates the probability of UCAVs being attacked or annihilated by the soft threat. Total soft threat fitness is referred to as the summation of all soft threat values, i.e.

$$Th\left(p(h)\right)=\sum_{j=1}^{M_2} Th_j\left(p(h)\right). \quad (14)$$

A lower soft threat fitness suggests a safer situation.

A threshold ζ for soft threats needs to be identified in advance, the value of which represents the tolerance degree of soft threats.

2.3.2.3 Collision Avoidance Constraints

In coordinated missions where multiple UCAVs are required, the collisions between the aerial vehicles must be avoided. To this end, there is a safe distance threshold R_{UAV}. And

$$C\left(p_{UAV^i},p_{UAV^j}\right)=\left(R_{UAV^i}+R_{UAV^j}\right)^2-\left\|p_{UAV^i}-p_{UAV^j}\right\|_2, \quad (15)$$

is defined as the collision function between UAV^i and UAV^j, where $\|\cdot\|_2$ represents 2-norm. Besides, no collision is guaranteed by assuring $C\left(p_{UAV^i},p_{UAV^j}\right)\leq 0$.

If UCAVs fly at the altitude-hold mode, which can be easily achieved by a control law, i.e.

$$u_3=-K_h\left(h-h_{des}\right), \quad (16)$$

where K_h is the proportional gain and h_{des} is a desired flight height), possible collisions can be eliminated by altering the flight height.

2.4 Objective Function

The objectives of trajectory planning of UCAV are:

1) to approach the center of LAR as much as possible;

2) to avoid hard threats in the battlefield;

3) and to maintain a safe distance from those soft threats.

The optimal trajectory planning of UCAVs can be transformed into

$$\min_{\left\{p_{UAV^i}(t),u_{UAV^i}(t)\right\}}\int_{t_0}^{t_f}\left[\varpi\sum_{i=1}^{N}\left\|p_{UAV^i}(t)-q_{T_i}(t)\right\|+\kappa\beta\sum_{i=1}^{N}Th\left(p_{UAV^i}(t)\right)\right]dt \quad (17)$$

In Eqn. (17), $q_{T_i}(t)=\left(\bar{x}_{T_i},\bar{y}_{T_i}\right)$ represents the center coordinate of LAR corresponding to UAV^i; ϖ and β indicate the weights of the first and third objective, $\varpi>\beta\geq 0$ and $\varpi+\beta=1$; $\kappa>0$ means a scaling factor for equalisation of the dimension of the two terms.

The complete constraints are listed as follows:

$$\begin{cases} V_{\min}\leq u_1^i\leq V_{\max} \\ a_{\min}\leq a\leq a_{mas} \\ \omega_{\min}\leq u_2^i\leq \omega_{\max} \\ \gamma_{\min}\leq u_3^i\leq \gamma_{\max} \\ r\geq r_{\min}=\dfrac{V}{\omega_{\max}} \\ F_j\left(p_{UAV^i}(t)\right)<0 \\ Th_j\left(p_{UAV^i}(h)\right)>\zeta \\ C\left(p_{UAV^{i_1}},p_{UAV^{i_2}}\right)\leq 0 \end{cases}, \quad (18)$$

$$i_1=1,\cdots,N,i_2=1,\cdots,N,i_1\neq i_2;j=1,\cdots M_1$$

For the purpose of simplification, a receding horizon approach is adopted, i.e.

$$\min_{\left\{p_{UAV^i}(t),u_{UAV^i}(t)\right\}}\int_{t_k}^{t_k+\delta}\left[\varpi\sum_{i=1}^{N}\left\|p_{UAV^i}(t)-q_{T_i}(t)\right\|+\kappa\beta\sum_{i=1}^{N}Th\left(p_{UAV^i}(t)\right)\right]dt, \quad (19)$$

where δ indicates the interval length of $[t_k,t_k+\delta\cdot\Delta t]$, and Δt refers to the time step. It is noteworthy that an excessive value of Δt can result in a poor solution accuracy.

3. CASE-BASED SOLUTION MODEL OF DELIVERY TRAJECTORY PLANNING

To solve the aforementioned trajectory planning problem, a novel and practical case-based method is put forward to achieve online planning in dynamic battlefields.

3.1 Key Parameters Identification

The current state vector of UAV^i at time k is

$$X_{UAV^i}(k)=\left[p_{UAV^i}^T(k)\,v_{UAV^i}^T(k)\right]^T=\begin{bmatrix}x_{UAV^i}(k) & y_{UAV^i}(k) & h_{UAV^i}(k) & v_{UAV^i}^x(k) \\ v_{UAV^i}^y(k) & v_{UAV^i}^h(k)\end{bmatrix}^T. \quad (20)$$

In convenience, UCAVs fly in the altitude-hold mode, i.e. $h_{UAV^i}(k)\equiv h_{UAV^i}$ and $v_{UAV^i}^h(k)\equiv 0$. Based on particle kinematics of UCAV, the potential ranges of heading angle and velocity after one time step are

$$Var_{\psi}^{UAV^i}=\left[\psi_{UAV^i}(k)+\omega_{\min}\cdot\Delta t,\psi_{UAV^i}(k)+\omega_{\max}\cdot\Delta t\right], \quad (21)$$

and

$$Var_{v}^{UAV^i}=\left[\max\left\{v_{UAV^i}+a_{\min}\cdot\Delta t,v_{\min}\right\},\min\left\{v_{UAV^i}+a_{\max}\cdot\Delta t,v_{\max}\right\}\right]. \quad (22)$$

The line-of-sight of UAV^i towards the center of LAR is

$$\varphi_{UAV^i}(k)=\tan^{-1}\left(\frac{\overline{y}_{T_i}(k)-y_{UAV^i}(k)}{\overline{x}_{T_i}(k)-x_{UAV^i}(k)}\right) \tag{23}$$

The furthest points used to predict whether UCAV is in danger for the next rolling time step can be calculated using Eqns. (24)-(25).

$$p^{TMAX}_{UAV^i}(k)=\left[x_{UAV^i}(k),y_{UAV^i}(k),h_{UAV^i}\right]^T + \frac{v_{UAV^i}(k)}{\omega_{\max}}\begin{bmatrix}\sin\left(\psi_{UAV^i}(k)+\frac{\pi}{2}\right)-\sin\left(\psi_{UAV^i}(k)\right)\\ -\cos\left(\psi_{UAV^i}(k)+\frac{\pi}{2}\right)+\cos\left(\psi_{UAV^i}(k)\right)\\ 0\end{bmatrix}, \tag{24}$$

and

$$p^{TMIN}_{UAV^i}(k)=\left[x_{UAV^i}(k),y_{UAV^i}(k),h_{UAV^i}\right]^T + \frac{v_{UAV^i}(k)}{\omega_{\min}}\begin{bmatrix}\sin\left(\psi_{UAV^i}(k)+\frac{\pi}{2}\right)-\sin\left(\psi_{UAV^i}(k)\right)\\ -\cos\left(\psi_{UAV^i}(k)+\frac{\pi}{2}\right)+\cos\left(\psi_{UAV^i}(k)\right)\\ 0\end{bmatrix}. \tag{25}$$

Namely, they are extreme points of UAV^i that can be reached at its current speed with the maximum and minimum turning rate.

Based on these variables, the possible situations of UAV^i after a time step can be predicted. Once the UCAV is predicted of possible encounter with threats, it needs to adjust its control variables immediately.

3.2 Threat Avoidance Strategy

Herein, the strategies applied to avoid hard and soft threats are introduced.

3.2.1 Hard Threat Avoidance Strategy

It is supposed that a hard threat $H_m=\langle A_m,P_m\rangle(m=1,\cdots,M_1)$ satisfies $F_m\left(p^{TMIN}_{UAV^i}(k)\right)\geq 0$ or $F_m\left(p^{TMAX}_{UAV^i}(k)\right)\geq 0$. This indicates a potential hard threat encounter of UAV^i. To avoid this, the acceptable variation range of the heading angle ought to be

$$Var^{UAV^i}_{\psi-H_m}(k)=\left[\psi^{H_m}_{UAV^i}(k)-\frac{\pi}{2},\psi^{H_m}_{UAV^i}(k)+\frac{\pi}{2}\right], \tag{26}$$

where $\psi^{H_m}_{UAV^i}(k)$ is one of the perpendicular directions to the tangential of the ellipse H_m at the point where this ellipse and the line through $p_{UAV^i}(h)$ and $A_m(h)$ intersect, which is closer to the direction of vector $\overrightarrow{A_m(h)p_{UAV^i}(h)}$. The approach of $\psi^{H_m}_{UAV^i}(k)$ is detailed[15].

Otherwise, if there is no indications that UAV^i is possible to encounter H_m, $Var^{UAV^i}_{\psi-H}(k)=[0,2\pi)$.

3.2.2 Soft Threat Avoidance Strategy

In response to soft threats, the UCAV is prohibited from flight through the area where the soft threat fitness value exceeds ζ. When $Th\left(p^{TMIN}_{UAV^i}(k)\right)\geq\zeta$ or $Th\left(p^{TMAX}_{UAV^i}(k)\right)\geq\zeta$, the acceptable variation range of the heading angle is

$$Var^{UAV^i}_{\psi-S}(k)=\left[\psi^{S}_{UAV^i}(k)-\frac{\pi}{2},\psi^{S}_{UAV^i}(k)+\frac{\pi}{2}\right], \tag{27}$$

where

$$\psi^{S}_{UAV^i}(k)=\tan^{-1}\left(\frac{-\partial Th(p)/\partial y}{-\partial Th(p)/\partial x}\Big|p=p_{UAV^i}(k)\right); \tag{28}$$

otherwise, $Var^{UAV^i}_{\psi-S}(k)=[0,2\pi)$.

3.3 Procedures of Trajectory Planning Strategy

Based on both threat models and mission demands, the situation of UCAVs falls into either of the following four cases.

Case 1: With the current velocity and heading angle, it is highly likely for the UCAV to encounter a hard threat. The vehicle should decelerate to the highest degree to turn as fast as possible.

Case 2: With the current velocity and heading angle, the UCAV is possible to encounter a highly risky area. The vehicle should decelerate to the highest degree to turn as fast as possible.

Case 3: Though there is neither hard nor soft threat posed to the UCAV, the distance between the vehicle and the center of LAR is not as close as required.

Case 4: Not only there is neither hard nor soft threat posed to the UCAV, the distance between the vehicle and the center of LAR is also close enough. In this case, the vehicle should make self-adjustment to satisfy the position and posture conditions for airborne bombs to be released.

To distinguish between the aforementioned cases, two control variables are introduced, as shown in the following equations.

$$Var^{UAV^i}_{CA}(k)=Var^{UAV^i}_{\psi-H_m}(k)\cap Var^{UAV^i}_{\psi}(k), \tag{29}$$

$$Var^{UAV^i}_{RH}(k)=Var^{UAV^i}_{CA}(k)\cap Var^{UAV^i}_{\psi-S}(k). \tag{30}$$

Besides the rules of the cases are summarised in Table 1.

Figure 2 provides the details of procedures of the proposed strategy. The computational time complexity of the proposed algorithm depends on the loop of threat cases classification. Suppose that for a UCAV, there are M waypoints and the total number of hard and soft threats is N. In the worst-case scenario, the complexity of the loop corresponds to the multiplication of M by the sum of all threats, i.e. $O(MN)$. The other component of the algorithm is $O(M)$. Consequently, the computational time complexity is $O(MN)$ for the proposed algorithm.

4. SIMULATION RESULTS AND ANALYSIS

The proposed planning strategy is validated using Matlab 2016b. The main hardware parameters of the computer are 4x Intel(R) Core(TM) i7 CPU @ 3.07GHz.

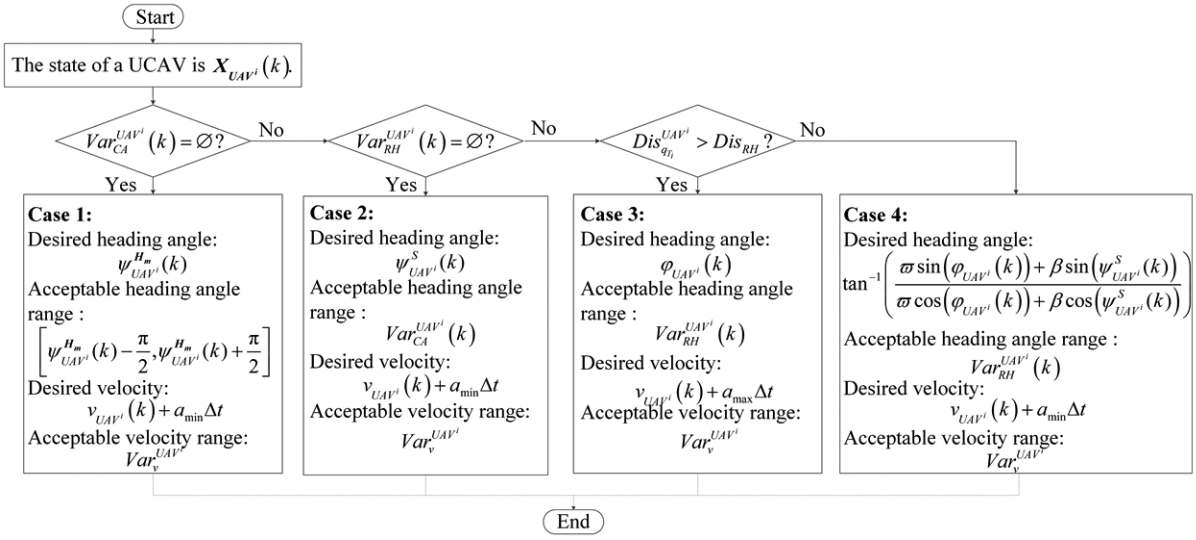

Figure 2. Flowchart of the case-based trajectory planning approach.

Table 1. Rules of the cases

Control variables	Serial number of cases
$Var_{CA}^{UAV^i}(k)=\varnothing$	1
$\begin{cases} Var_{CA}^{UAV^i}(k)\neq\varnothing, \\ Var_{RH}^{UAV^i}(k)=\varnothing \end{cases}$	2
$\begin{cases} Var_{CA}^{UAV^i}(k)\neq\varnothing, \\ Var_{RH}^{UAV^i}(k)\neq\varnothing, \\ Dis_{q_{Ti}}^{UAV^i}(k)> Dis_{RH} \end{cases}$	3
$\begin{cases} Var_{CA}^{UAV^i}(k)\neq\varnothing, \\ Var_{RH}^{UAV^i}(k)\neq\varnothing, \\ Dis_{q_{Ti}}^{UAV^i}(k)\leq Dis_{RH} \end{cases}$	4

Table 2. Initial state of hard threats

Threats number	Position of center point (km)	Radius (km)	Height *h* (km)
1	(13,17)	1	2
2	(5,9)	1.5	1.5
3	(13,4)	1	1.7
4	(10,10)	1	1
5	(6,16)	1.5	2

Table 3. Motion constraints of the UCAV

Constraints	Values (Ranges)
Velocity $[V_{\min}, V_{\max}]$/(km/s)	$[0.082, 0.59]$
Acceleration/ (km/s^2)	$[-0.005, 0.005]$
Turning rate/(°/s)	$[-20, 20]$
$h_{\max}$ /km	12
Heading angle/(°)	$[-180, 180]$

4.1 Simulation Settings

The UCAV adopted in simulations is the Storm Shadow UCAV. The relevant platform parameters are listed[15].

Airborne reconnaissance sensors are capable of providing the position and shape of all pop-up mobile threats and targets instantly. The effective maximum detection distance is set to 20 km.

The battlefield is a $20km\times20km$ square area where five hard threats (shadow round area) and five soft threats (yellow solid-line-bounded circle) are located. The contour demonstrates the total soft threat value as calculated using Eqn. (15).

The information about key parameters is summarised in Table 3.

In the simulation, the initial speed and heading angle of the UCAV are set to 0.2 km/s and 135° respectively. The distance threshold between the vehicle and the center of LAR is set to 1 km, while the maximum release velocity required for launching airborne bombs is set to 0.16 km/s. The acceptance threshold for soft threats is set to 0.5, and $\varpi=\beta=0.5$. The initial time is $t_0=0$ and $\Delta t=1s$.

4.2 Scenario 1: Stationary Threats

In Scenario 1, a UCAV initially at (2 km, 3 km, 1.5 km) and a target at (14 km, 14 km, 0 km) are applied in the battlefield.

The trajectory based on the proposed case-based online planning strategy is illustrated in Fig. 3. The runtime of simulation is 19.69s. The total flight time is 104s.

The flight path generated by the planning strategy is smooth and the success in averting the threats is achieved. The ballistic trajectory of guided bombs after launch is denoted as a bold blue line. During the flight, the vehicle remains at a relatively stable altitude. In the meantime, the distance between the terminal launching point and the center of LAR is 0.3482 km and the release velocity is 0.15 km/s, which meets the release condition of airborne bombs.

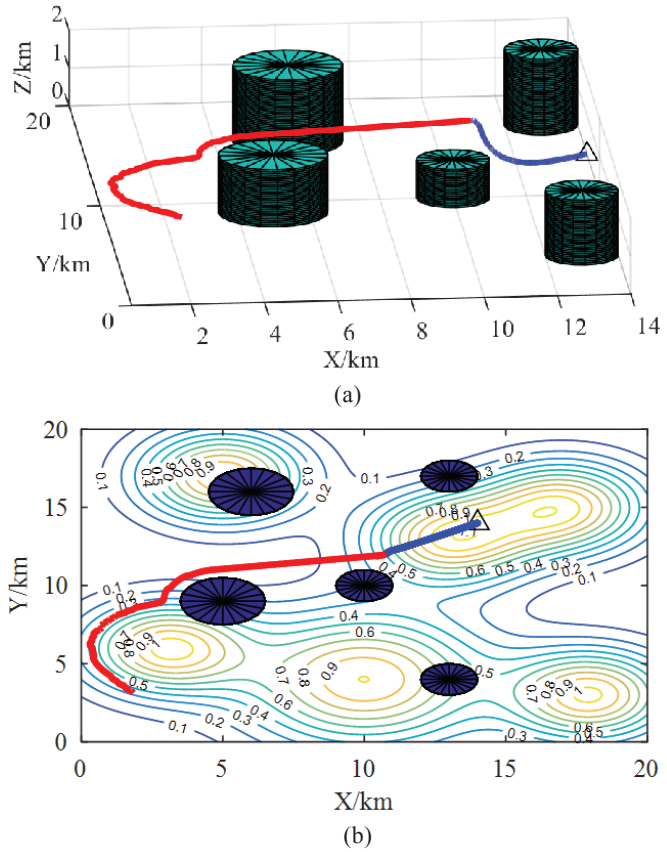

Figure 3. Real-time trajectory of UCAV delivering ground-attack bombs: (a) 3D trajectory (b) 2D trajectory.

The variation of control variables and relative distance are depicted in Fig. 4.

4.3 Scenario 2: Pop-up Mobile Threat and Single Mobile Target

In this scenario, the performance of the proposed planning strategy is validated with a mobile target moving northwest at a speed 0.03 km/s and a pop-up mobile threat.

The simulation is conducted without predicting the positions of the target. As a result, for each time of iteration, the planning strategy uses the snapshot position of mobile targets and threats, which transforms the planning problem in a dynamic environment into an instantaneous static problem.

The trajectory is shown in Fig. 5, and the total flight time is 113 s.

As indicated by the simulation results obtained in Scenario 2 (Fig. 6), the proposed online case-based trajectory planning strategy is well suited to the complex battlefield with pop-up threats and mobile ground targets.

In the first 44 s, the vehicle makes adjustment to its heading angle and velocity on a continued basis to fly along the contour of threats. During the flight towards the target, once the UCAV approaches the highly risky regions, it decelerates and turns its heading to run away, which causes the fluctuation of the control variables. At the time of 69 s, the UCAV achieves a success in avoiding Threat 2 and locates at a low risk region, before accelerating towards the target. After 11 s of acceleration, the UCAV detects a pop-up mobile threat,

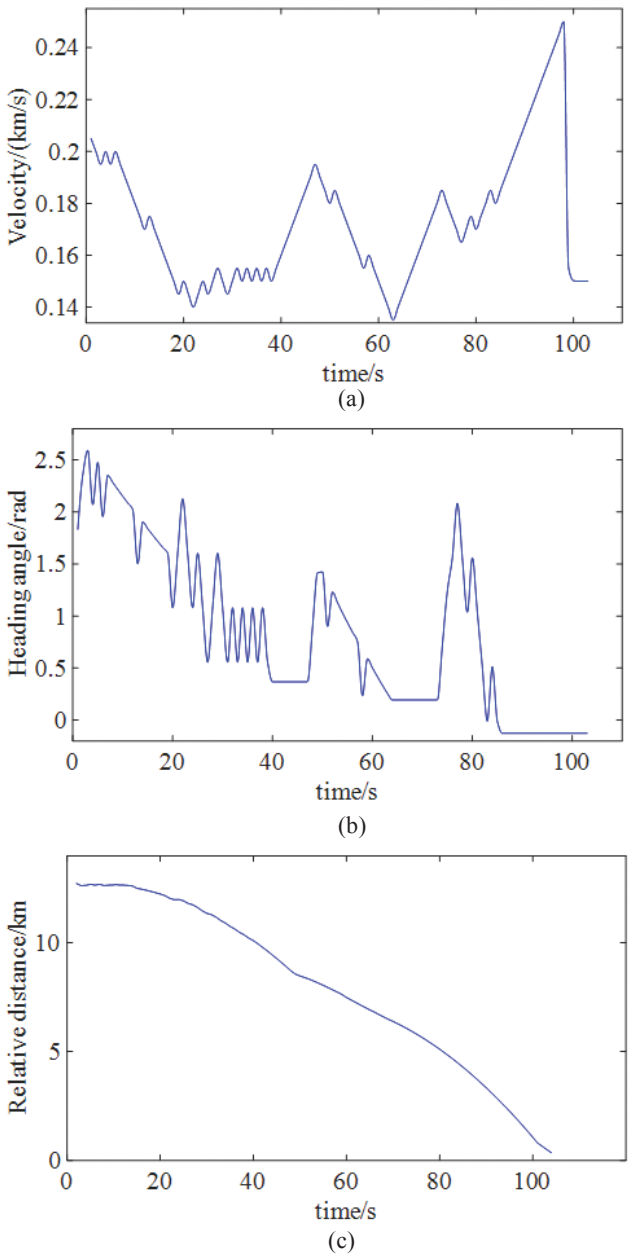

Figure 4. Variation of relevant flight parameters (a) Variation of velocity, (b) Variation of heading angle, and (c) Relative distance.

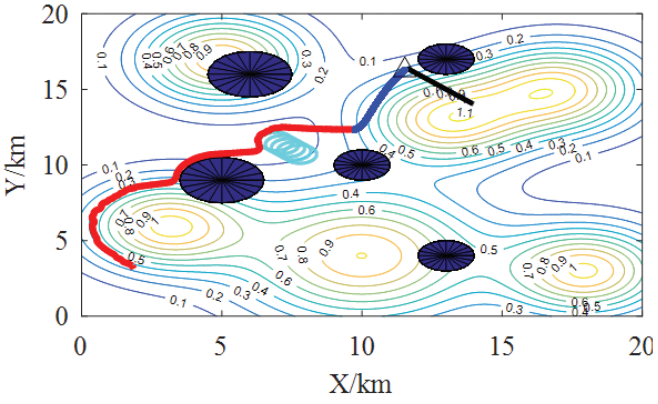

Figure 5. Real-time 2D trajectory of UCAV.

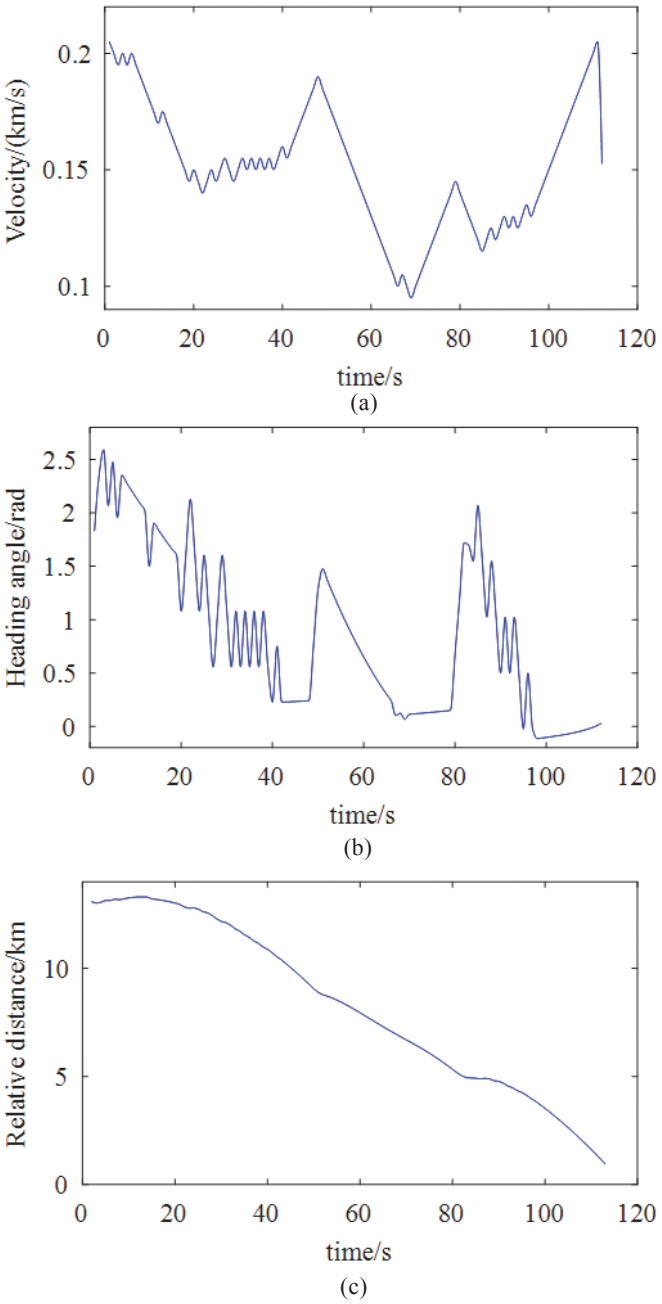

Figure 6. Variation of control variables and relative distance in Scenario 2: (a) Variation of velocity, (b) Variation of heading angle, and (c) Variation of relative distance.

which triggers deceleration and alter to turn its heading for the avoidance of it. At the time of 99 s, the UCAV averts the pop-up threat with success and carries on flying towards the center of LAR.

4.4 Computational Burden

In order to see whether the changes in the time horizon (Δt herein) for guidance have an impact on the final trajectory, the runtime, mission completion time, final relative distance of the algorithm are compared with different time steps. In this scenario, the UCAV initially locates at 17 km, 1 km, 2 km and the target locates at 3 km, 19 km, 0 km. The kinematic parameters of the UCAV remain the same as in Section 4.1.

The comparison results are presented in Table 4. From Table 4, it can be seen that with different Δt, the UCAV can manage to survive both hard and soft threats. Therefore, the main selective factor of Δt is the acceptable computational burden. In some exceptional circumstances with a large tolerance of computational burden, such as short-distance sudden assault and highly risky battlefields with a large density of threats, a smaller Δt is preferred. Under normal circumstances, it is recommended that Δt ranges between 1s and 5s in consideration of the tradeoff made between the collision avoidance and computational burden.

The online trajectory planning algorithm is suitable for dynamic scenarios where pop-up mobile threats move at a similar speed. If the threat moves at a faster pace than the vehicle, the algorithm may be unable to respond promptly, which could strict the application of the algorithm in an air-to-ground attack mission without considering supersonic threats.

Table 4. Comparison results with different time steps

Time step Δt	Terminal relative distance (km)	Algorithm runtime (s)	Total flight time (s)	Average time for a step(s)
0.5	0.4879	53.85	125	0.4308
1	0.4926	25.23	131	0.1926
2	0.4352	13.81	124	0.1114
5	0.1785	8.51	190	0.0448

5. CONCLUSIONS

This paper concentrates on obtaining on-board trajectories for UCAVs executing ground attack missions. Allowing for the complex battlefields with obstacles, no-fly zones and air defense threats, the optimal control problem of trajectory planning has been transformed into the situation classification of four cases.

The main contributions of the papers are summarised as follows. Firstly, the trajectory planning problem of UCAVs with airborne guided bombs is mathematically formulated as a traditional optimal control problem (OCP). In order to meet the release conditions of guided bombs, the LAR is integrated into the planning constraints. Secondly, a case-based planning strategy in combination with the receding horizon method is proposed to achieve real-time trajectories for UCAVs to deliver airborne bombs.

To conduct a further research, the proposed online trajectory planning strategy is recommended to be combined with some representative computational intelligence algorithms, such as monarch butterfly optimisation (MBO) algorithm[17], earthworm optimisation algorithm[18] (EWA) and elephant herding optimisation (EHO) algorithm[19], which is conductive to solving the global optimisation problems effectively, while ensuring the missions with large-scale battlefields can be accommodated.

REFERENCES

1. Liu, J.-J.; Wang, W.-P.; Li, X.-B.; Wang, T. & Wang, T.-Q. A motif-based mission planning method for UAV swarms considering dynamic reconfiguration. *Def. Sci. J.*, 2018, **68**(2), 159-166. doi: 10.14429/dsj.68.11959
2. Goerzen, C.; Kong, Z. & Mettler, B. A survey of motion planning algorithms from the perspective of autonomous UAV guidance. *J. Intell. Robot. Syst.*, 2010, **57**, 65–100. doi: 10.1007/s10846-009-9383-1
3. Wang, G.-G.; Guo, L.-H.; Duan, H.; Wang, H.-Q. Luo, L. & Shao M.-Z. A hybrid meta-heuristic DE/CS algorithm for UCAV three-dimension path planning. *Sci. World J.*, 2012, 1–11. doi: 10.1100/2012/583973
4. Wang, G.-G. Moth search algorithm: a bio-inspired metaheuristic algorithm for global optimisation problems. *Memet. Comp.* 2016. doi: 10.1007/s12293-016-0212-3
5. Xu, C.-F.; Duan, H.-B. & Liu, F. Chaotic artificial bee colony approach to uninhabited combat air vehicle (UCAV) path planning. *Aerosp Sci. Technol*., 2010, **14**, 535–541. doi:10.1016/j.ast.2010.04.008
6. Wang, G.-G.; Guo, L.-H.; Duan, H.; Liu, L.; Wang, H.-Q. & Shao M.-Z. Path planning for uninhabited combat aerial vehicle using hybrid meta-heuristic DE/BBO algorithm. *Adv. Sci., Eng. Med.*, 2012, **4**(6), 550–564. doi: 10.1166/asem.2012.1223
7. Duan, H.-B.; Liu, S.-Q. & Wu, J. Novel intelligent water drops optimization approach to single UCAV smooth trajectory planning. *Aerosp Sci. Technol*., 2009, **13**(8), 442–449. doi: 10.1016/j.ast.2009.07.002
8. Wang, G.-G.; Chu, H.-C. & Mirjalili, S. Three-dimensional path planning for UCAV using an improved bat algorithm. *Aerosp Sci. Technol*., 2016, **49**, 231-238. doi: 10.1016/j.ast.2015.11.040
9. Betts, J.T. Survey of numerical methods for trajectory optimization. *J. Guid Control Dyn.*, 1998, **21**(2), 193-207. doi: 10.2514/2.4231
10. Zhang, Y.; Chen, J. & Shen, L.-C. Real-time trajectory planning for UCAV air-to-surface attack using inverse dynamics optimization method and receding horizon control. *Chi. J. Aeronaut.*, 2013, **26**(4), 1038–1056. doi: 10.1016/j.cja.2013.04.040
11. Zhu, W.-R. & Duan, H.-B. Chaotic predator-prey biogeography-based optimization approach for UCAV path planning. *Aerosp Sci. Technol*., 2014, **32**, 153-161. doi: 10.1016/j.ast.2013.11.003
12. Duan, H.-B. & Huang, L.-Z. Imperialist competitive algorithm optimized artificial neural networks for UCAV global path planning. *Neurocomputing*, 2014, **125**, 166-171. doi: 10.1016/j.neucom.2012.09.039
13. Curiac, D.I. & Volosencu, C. Path planning algorithm based on Arnold cat map for surveillance UAVs. *Def. Sci. J.*, 2015, **65**(6), 483-488. doi: 10.14429/dsj.65.8483
14. Wilson, S.A.; Vultetich, I.J.; Fletcher, D.; Jokic, M.; Brett, M.; Boyd, C.; Williams, W. & Bryce, I. Guided weapon danger area & safety template generation-a new capability. *In* AIAA Atmospheric Flight Mechanics Conference and Exhibit, 2008. doi: 10.2514/6.2008-7123
15. Jiang, H. & Liang, Y.-Q. Online path planning of autonomous UAVs for bearing-only standoff multi-target following in threat environment. *IEEE Access*, 2018, **6**, 22531-22544. doi: 10.1109/ACCESS.2018.2824849
16. Storm Shadow UCAV performance. Available from: http://www.aerospaceweb.org/design/ucav/main.html.
17. Wang, G.-G.; Deb, S. & Cui, Z.-H. Monarch butterfly optimization. *Neural Comput. Appl.*, 2019, **31**(7), 1995-2014. doi: 10.1007/s00521-015-1923-y
18. Wang, G.-G.; Deb, S. & Coelho, L.S. Earthworm optimization algorithm: a bio-inspired metaheuristic algorithm for global optimization problems. *Int. J. Bio-Inspired Comput.*, 2015, **12**, 1-22. doi: 10.1504/IJBIC. 2015.10004283
19. Wang, G.-G.; Deb, S.; Gao, X.-Z. & Coelho, L.S. A new metaheuristic optimization algorithm motivated by elephant herding behavior. *Int. J. Bio-Inspired Comput.*, 2016, **8**(6), 394. doi: 10.1504/IJBIC.2016.10002274

CONTRIBUTORS

Ms Jiayu Tang is currently pursuing her PhD in Naval Aviation University, Yantai, China. Her research interests include: cooperative task assignment and path planning of multi-UAV.
In the current study, she has done simulation, post processing of the results and preparation of the manuscript.

Prof. Xiangmin Li obtained his PhD from Northwestern Polytechnical University. He is currently a professor and a doctoral supervisor in Naval Aviation University, China. His research interests include: Fire command and control.
In the current study, he has provided guidance in examining the results and reviewed the final manuscript .

Dr Jinjin Dai received his PhD (weapon systems and application engineering) in 2012 from Naval Aviation University. He is currently a lecturer in Naval Aviation University, China. His research interests include: Fire command and control.
In the current study, he has provided guidance in executing the battlefield modelling and the simulation.

Dr Ning Bo received his PhD (weapon systems and application engineering) in 2018 from Naval Aviation University. He is currently an engineer in Unit 91213 of PLA, Yantai, China. His research interests include: Weapon system simulation.
In the current study, he has provided guidance in the solution of LAR.